

# Preparation and photoelectrochemical characterization of a red sensitive osmium complex containing 4,4',4''-tricarboxy-2,2':6',2''-terpyridine and cyanide ligands

Roberto Argazzi<sup>a,\*</sup>, Gerardo Larramona<sup>b</sup>, Cristiano Contado<sup>c</sup>, Carlo Alberto Bignozzi<sup>c,\*</sup>

<sup>a</sup> *Istituto per la Sintesi Organica e la Fotoreattività (ISOF—CNR), sezione di Ferrara, Via Luigi Borsari 46, 44100 Ferrara, Italy*

<sup>b</sup> *IMRA Europe S.A.S., 220 rue Albert Caquot, 06904 Sophia Antipolis, France*

<sup>c</sup> *Dipartimento di Chimica, Università di Ferrara, Via Luigi Borsari 46, 44100 Ferrara, Italy*

Received 25 September 2003; received in revised form 10 December 2003; accepted 10 December 2003

Dedicated to Prof. Shozo Yanagida in recognition of his achievements.

## Abstract

The complex ion  $[\text{Os}^{\text{II}}(\text{H}_3\text{tcterpy})(\text{CN})_3]^-$  ( $\text{H}_3\text{tcterpy} = 4,4',4''\text{-tricarboxy-2,2':6',2''-terpyridine}$ ) has been prepared by an easy methodology and characterized. The UV-Vis absorption in  $\text{CH}_3\text{OH}$  shows a series of MLCT bands with distinct maxima spanning the whole visible spectrum and a remarkably intense band ( $\epsilon \approx 1500 \text{ M}^{-1} \text{ cm}^{-1}$ ) at 811 nm associated to a spin-forbidden singlet–triplet MLCT transition allowed by spin–orbit coupling. Cyclic voltammetry of the complex in  $\text{CH}_3\text{OH}$  showed a reversible  $\text{Os}^{\text{II}} \rightarrow \text{Os}^{\text{III}}$  oxidation process with  $E_{1/2} = 663 \text{ mV}$ . Controlled shifting of MLCT absorption and Os oxidation potential is accomplished by simply changing the degree of protonation of the carboxylic groups. The behavior of the complex as sensitizer in dye sensitized solar cells (DSSCs) has been tested giving satisfactory IPCE values and showing contribution to the photoaction spectrum from the singlet to triplet transition. The photochemical stability was qualitatively investigated and proved to be better than that of the best Ru-based sensitizer known up to now. © 2004 Elsevier B.V. All rights reserved.

**Keywords:** Osmium; Terpyridine; Sensitizer; DSSC

## 1. Introduction

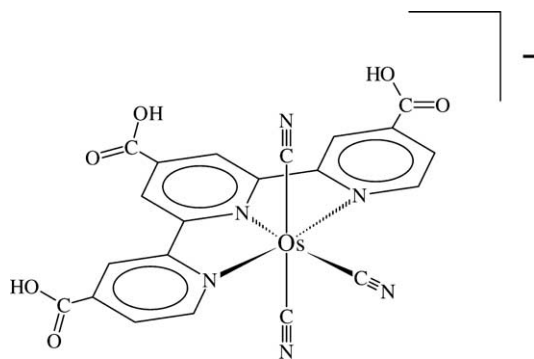
In the past 15 years there has been much interest to increase the stability and performances of the dye sensitized solar cells (DSSCs) developed by the research group of Hagfeldt and Graetzel [1]. Transition metal charge transfer complexes have been successfully employed as sensitizers of photoanodes based on wide band-gap semiconductors, which represent a key component of the DSSC. Despite the fact that these dyes can exhibit photochemical instability or irreversible electrochemistry, with ligand substitution reactions taking place from the one-electron oxidized form [2], a remarkable stability was observed in long term experiments on sealed DSSCs [3]. This unique feature is due to a peculiar series of electron transfer processes which occur in the DSSCs, and in particular to ultrafast charge injection from the electronically excited dye [4–6] and to fast reduction of the nascent oxidized dye by an electron transfer me-

diator [7–9], normally dissolved in the electrolyte solution. Recently, attention has been paid to the preparation of solid state hole transfer mediators [10,11] which are obviously of great interest, since allow an easy fabrication of the DSSC, but may have as drawback the fact that have a high resistance and do not provide a homogeneous and intimate contact with the dye molecule adsorbed on the mesoporous semiconductor. These features can be responsible for the slow reduction of the oxidized form of the dye, with consequent decomposition. It can be foreseen, therefore, that a long term stability of solid state DSSCs will require the use of dye molecules exhibiting a good stability in their oxidized forms.

Previous studies by the Lewis group [12,13] have shown that osmium complexes containing the 4,4'-dicarboxylic acid 2,2'-bipyridine ligand display a reversible electrochemistry and allow at the same time to extend the spectral response of  $\text{TiO}_2$  photoanodes, providing photocurrents and external quantum yields comparable to those of analogous ruthenium complexes. In this paper, we wish to report the preparation and characterization of the  $[\text{Os}^{\text{II}}(\text{H}_3\text{tcterpy})(\text{CN})_3](\text{TBA})$  complex (Scheme 1) ( $\text{H}_3\text{tcterpy} = 4,4',4''\text{-tricarboxy-2,2':6',2''-terpyridine}$ ), normally dissolved in the electrolyte solution.

\* Corresponding authors.

E-mail address: [agr@unife.it](mailto:agr@unife.it) (R. Argazzi).



Scheme 1.

6',2''-terpyridine, TBA = tetrabutylammonium), and of its differently protonated species which were found to exhibit a reversible electrochemical behavior as well as photochemical stability and a considerable red sensitivity.

## 2. Experimental

### 2.1. Materials

The following chemicals were purchased and used without further purification:  $(\text{NH}_4)_2\text{Os}^{\text{IV}}\text{Cl}_6$  (Alfa Aesar, Johnson Matthey), TBAOH (40 wt.% solution in water, Aldrich), TBACN (Fluka). The ligand 4,4',4''-tricarboxy-2,2':6',2''-terpyridine ( $\text{H}_3\text{tcterpy}$ ) was available from previous studies.  $(\text{TBA})_2\text{Os}^{\text{IV}}\text{Cl}_6$  was precipitated by addition of TBACl (Fluka) to an aqueous solution of  $(\text{NH}_4)_2\text{Os}^{\text{IV}}\text{Cl}_6$ . The complex  $[\text{Ru}^{\text{II}}(\text{H}_3\text{tcterpy})(\text{NCS})_3]^-$  was either available from previous studies or prepared by the synthetic procedure followed for the osmium complex (Section 2.4). Solvents used in synthesis were of reagent grade while those for spectroscopic measurements were UV grade (Fluka). Chromatographic purification was performed by gel permeation on Sephadex LH20 (Pharmacia). Electrodes for the dye sensitized cells were cut from fluorine-doped tin oxide (FTO) conducting glass sheets of 1 mm thickness with a surface resistivity of  $10 \Omega/\text{m}^2$  (Nippon Sheet Glass).

### 2.2. Apparatus and procedures

$^1\text{H}$  NMR spectra were recorded at 300 MHz and  $25^\circ\text{C}$  on a Varian Gemini 300 spectrometer. Infrared spectra were taken in KBr pellets at a resolution of  $6 \text{ cm}^{-1}$  using a Bruker IFS-88 FT-IR spectrophotometer. UV-Vis spectra were recorded on a Perkin-Elmer Lambda 40 spectrophotometer. Linear sweep cyclic voltammetry experiments were carried out with an Autolab PGSTAT30 potentiostat/galvanostat, using a conventional three electrode cell equipped with a glassy carbon working electrode, an SCE reference electrode and a platinum counter electrode. Irradiation experiments were performed with a 150 W Xe arc

lamp (Osram) through a 400 nm cut-off filter. Photoelectrochemical performances of the complexes were evaluated on sandwich type cells consisting of a photoanode, with an active area of  $0.54 \text{ cm}^2$ , a counter electrode of platinumized FTO conducting glass and  $\text{LiI } 2 \text{ M}/\text{I}_2 \text{ 0.1 M}$  in  $\gamma$ -butyrolactone as electrolyte. The spectral response or incident photon to current efficiency (IPCE) measurements were carried out with an in-house test bench controlled by computer, which mainly consisted on the following items: a high power (450 W) xenon short-arc ozone free lamp OSRAM xenon connected to a power supply Jobin Yvon, a large output monochromator TRIAX-180 Jobin Yvon, two high-pass filters (320 and 590 nm) used to cut high orders wavelengths, a bi-concave lens BK7 from Melles Griot ( $f$ : 127 mm; diameter: 50 mm), and two multimeters Keithley 199 used to measure the short-circuit current of the reference and the test cells. The reference cell was a silicon diode Melles Griot 13 DSI 011 of 1 cm diameter and it was calibrated versus the wavelength from 400 to 1100 nm. The IPCE software calculated the integrated current corresponding to the solar standard spectrum AM1.5G by using the IPCE spectrum and the solar standard in the interval 400–1100 nm. The cell irradiance in the IPCE test bench was of the order of  $100 \text{ W}/\text{m}^2$  in the whole wavelength interval.

### 2.3. Preparation of $\text{TiO}_2$ films

Nanocrystalline transparent  $\text{TiO}_2$  films were obtained from a colloidal suspension of  $\text{TiO}_2$  similar to those prepared as described elsewhere [14]. The suspension was spread out on the conducting glass by gently pressing a glass slide, with a rectified edge, onto a pair of 3 M scotch tape strips separated by the desired length, and smoothly drawing it to obtain a uniform layer filling the gap between the strips. After drying at room temperature, the tape was removed and the electrodes were fired in an oven at  $450^\circ\text{C}$  for 30 min. Film thickness were in the range 16–18  $\mu\text{m}$ , and looked white opaque, so increasing the light scattering property. Adsorption of the dye was accomplished by dipping the electrodes still hot ( $70$ – $80^\circ\text{C}$ ) in a  $5 \times 10^{-4} \text{ M}$  solution of the complex in  $\text{CH}_3\text{OH}$  and letting them immersed in the solution at room temperature for 24 h. Dye sensitized electrodes were kept in a desiccator on silica gel.

### 2.4. Synthesis

#### 2.4.1. $[\text{Os}^{\text{II}}(\text{H}_3\text{tcterpy})(\text{CN})_2(\text{CNH})]$

To a suspension of 253 mg (0.69 mmol) of  $\text{H}_3\text{tcterpy}$  in 40 ml of *n*-butanol, 615 mg (0.69 mmol) of  $(\text{TBA})_2\text{Os}^{\text{IV}}\text{Cl}_6$  were added and the mixture was heated to reflux. An excess of TBACN (2.8 g, 10 mmol) was then added and the mixture was left refluxing for 6 h. Evaporation to dryness yielded a brown solid that was dissolved in the minimum volume of water at  $\text{pH} = 8$  adding aqueous TBAOH 0.1 M. To this solution, 2 M HCl was carefully added dropwise

under an efficient fume cupboard until the pH was about 1. Stripping of HCN was helped bubbling argon. The resulting greenish–brown precipitate was filtered off and dried. The solid was dissolved in  $10^{-3}$  M HCl/CH<sub>3</sub>OH and loaded on a Sephadex LH20 column. Elution was performed with  $10^{-3}$  M HCl/CH<sub>3</sub>OH. The first dark brown main fraction was collected and evaporated to dryness yielding the neutral complex [Os<sup>II</sup>(H<sub>3</sub>tcterpy)(CN)<sub>2</sub>(CNH)]. <sup>1</sup>H NMR [Os(H<sub>3</sub>tcterpy)(CN)<sub>3</sub>] (H) (300 MHz, CD<sub>3</sub>OD)  $\delta$  ppm: 8.01 (2H, dd, H<sup>5,5''</sup>), 8.94 (2H, s, H<sup>3,3''</sup>), 9.04 (2H s, H<sup>3',5'</sup>), 9.24 (2H, d, H<sup>6,6''</sup>). Analysis calculated for [Os(H<sub>3</sub>tcterpy)(CN)<sub>2</sub>(CNH)]  $\times$  3H<sub>2</sub>O: C = 36.63%, N = 12.20%, H = 2.62%, found: C = 36.64%, N = 11.91%, H = 2.59%.

#### 2.4.2. [Os<sup>II</sup>(H<sub>2</sub>tcterpy)(CN)<sub>3</sub>](TBA)<sub>2</sub>

This complex was prepared by addition of two equivalents of TBAOH to a solution of [Os<sup>II</sup>(H<sub>3</sub>tcterpy)(CN)<sub>2</sub>(CNH)] in CH<sub>3</sub>OH. <sup>1</sup>H NMR (300 MHz, CD<sub>3</sub>OD)  $\delta$  ppm: 1.05 (24H, t, CH<sub>3</sub>), 1.42 (16H, m, CH<sub>2</sub>), 1.65 (16H, m, CH<sub>2</sub>), 3.25 (12H, t, CH<sub>2</sub>), 7.93 (2H, dd, H<sup>5,5''</sup>), 8.84 (2H, s, H<sup>3,3''</sup>), 8.88 (2H s, H<sup>3',5'</sup>), 9.38 (2H, d, H<sup>6,6''</sup>).

#### 2.4.3. [Os<sup>II</sup>(Htcterpy)(CN)<sub>3</sub>](TBA)<sub>3</sub>

This complex was prepared by addition of three equivalents of TBAOH to a solution of [Os<sup>II</sup>(H<sub>3</sub>tcterpy)(CN)<sub>2</sub>(CNH)] in CH<sub>3</sub>OH. <sup>1</sup>H NMR (300 MHz, CD<sub>3</sub>OD)  $\delta$  ppm: 1.02 (36H, t, CH<sub>3</sub>), 1.40 (24H, m, CH<sub>2</sub>), 1.68 (24H, m, CH<sub>2</sub>), 3.22 (24H, t, CH<sub>2</sub>), 7.92 (2H, dd, H<sup>5,5''</sup>), 8.84 (2H, s, H<sup>3,3''</sup>), 8.88 (2H, s, H<sup>3',5'</sup>), 9.38 (2H, d, H<sup>6,6''</sup>).

### 3. Results and discussion

The formulation of the complex [Os<sup>II</sup>(H<sub>3</sub>tcterpy)(CN)<sub>2</sub>(CNH)] as a neutral species with one protonated cyanide has been confirmed by elemental analysis, <sup>1</sup>H NMR and FT-IR. The NMR spectrum is consistent with C<sub>2v</sub> symmetry and shows the characteristic signals of the coordinated H<sub>3</sub>tcterpy ligand in the aromatic region and the absence of any TBA cation in the aliphatic region, according to the elemental analysis findings. The presence of one protonated cyanide is directly demonstrated by the comparison of the FT-IR spectrum of [Os<sup>II</sup>(H<sub>3</sub>tcterpy)(CN)<sub>2</sub>(CNH)] with that of [Os<sup>II</sup>(H<sub>2</sub>tcterpy)(CN)<sub>3</sub>](TBA)<sub>2</sub> in KBr pellets (Fig. 1). The spectrum of the anionic species shows a single band, due to CN stretching with a maximum at 2076 cm<sup>-1</sup>, which is also observed in the spectrum of the neutral complex together with a second band, of lower intensity, at 2000 cm<sup>-1</sup>. This lower energy band can be assigned to the protonated cyanide [15] and can be explained in terms of an increased back-donation from the Os d $\pi$  orbitals to the  $\pi^*$  orbitals of CN–H, which lowers the C–N bond order. The expected intensity ratio 1:2 ( $\nu_{\text{CN}}(2000):\nu_{\text{CN}}(2076)$ ) was found for the two bands and supports this assignment. Furthermore, the characteristic group of bands of the TBA<sup>+</sup>

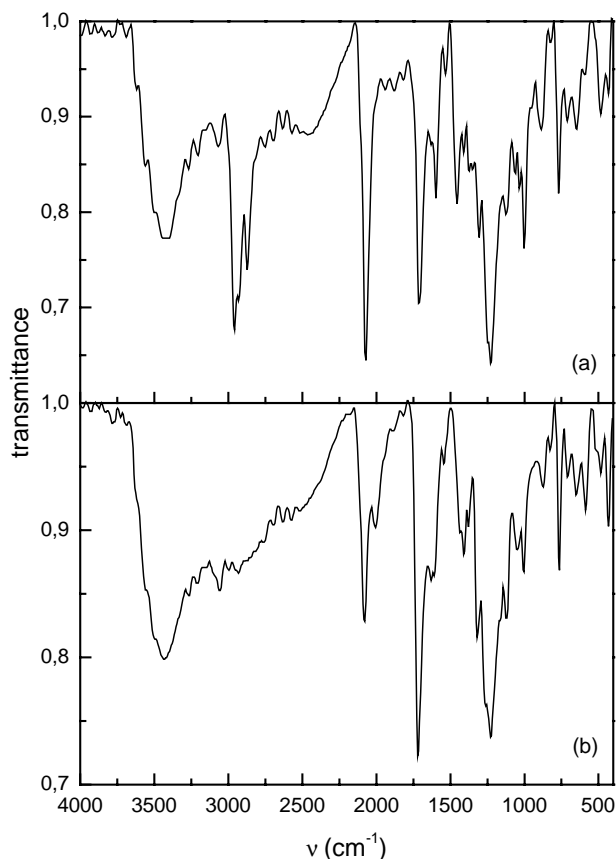


Fig. 1. FT-IR spectra in KBr pellets of (a) [Os<sup>II</sup>(H<sub>2</sub>tcterpy)(CN)<sub>3</sub>](TBA)<sub>2</sub> and (b) [Os<sup>II</sup>(H<sub>3</sub>tcterpy)(CN)<sub>2</sub>(CNH)].

cation in the region 2800–3000 cm<sup>-1</sup> found in the spectrum of [Os<sup>II</sup>(H<sub>2</sub>tcterpy)(CN)<sub>3</sub>](TBA)<sub>2</sub> is completely absent in that of the neutral species.

#### 3.1. UV-Vis absorption

The UV-Vis absorption spectrum in the wavelength interval 200–900 nm of the species [Os<sup>II</sup>(H<sub>3</sub>tcterpy)(CN)<sub>2</sub>(CNH)] in CH<sub>3</sub>OH is reported in Fig. 2. This electronic spectrum shows two bands in the UV region at 291 and 336 nm due to  $\pi$ – $\pi^*$  transitions localized on the H<sub>3</sub>tcterpy ligand, a series of four regularly spaced bands with decreasing intensity and distinct maxima at 394, 467, 531 and 607 nm assignable to Os  $\rightarrow$  H<sub>3</sub>tcterpy metal to ligand charge transfer transitions (MLCT) and a single broad feature at 811 nm which can be attributed to a spin-forbidden singlet–triplet MLCT [16]. This last transition, of remarkable intensity ( $\epsilon \approx 1500 \text{ M}^{-1} \text{ cm}^{-1}$ ), is allowed by the large spin–orbit coupling constant of osmium (3200 cm<sup>-1</sup>) [17]. For complexes of the types [Os<sup>II</sup>(bpy)<sub>2</sub>(X<sub>2</sub>)] (bpy = 2, 2'-bipyridine; X = Cl<sup>-</sup>, NCS<sup>-</sup>, pyridine, triphenylphosphine) has been reported that the <sup>3</sup>MLCT state is indeed 30% singlet in character [16] due to the mixing caused by spin–orbit interaction. The number of bands observed in the visible region can be rationalized in terms of symme-

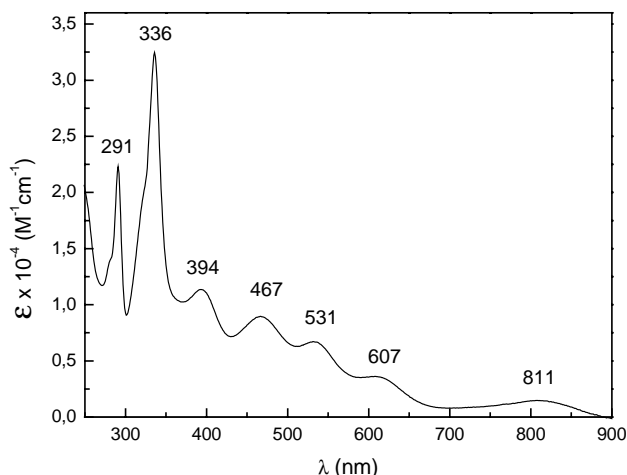


Fig. 2. UV-Vis spectrum of  $[\text{Os}^{\text{II}}(\text{H}_3\text{tcterpy})(\text{CN})_2(\text{CNH})]$  in  $\text{CH}_3\text{OH}$ .

try arguments as schematically pictured in the qualitative diagram of Fig. 3. The relative order of the  $d_{xz}$ ,  $d_{xy}$ , and  $d_{yz}$  orbitals is dictated by the  $C_{2v}$  symmetry of the complex and by the mixing of these orbitals with the  $\pi^*$  orbitals of the tcterpy ligand and the ligand group orbitals of the

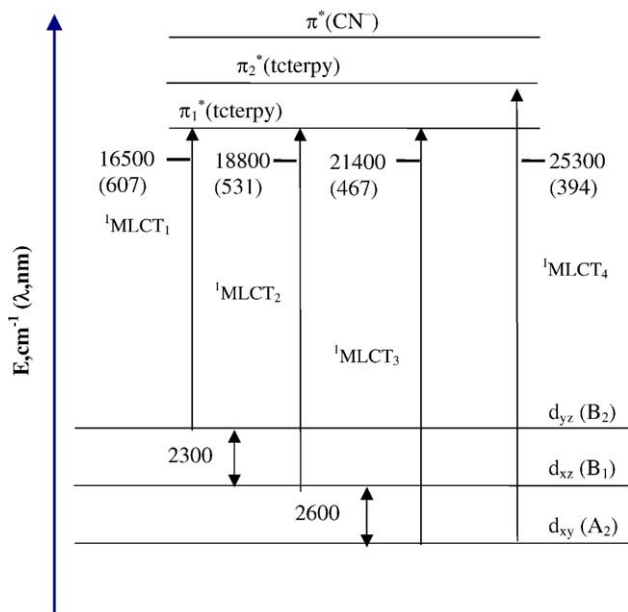
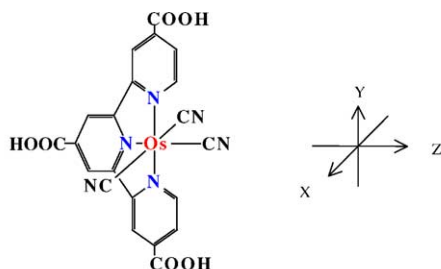


Fig. 3. Qualitative energy level diagram for the complex  $[\text{Os}^{\text{II}}(\text{H}_3\text{tcterpy})(\text{CN})_3](\text{TBA})$ .

three cyanide, of symmetry  $A_2$ ,  $B_1$ , and  $B_2$  [18]. The three bands observed in the wavelength interval 450–700 nm can be therefore assigned to the transitions  ${}^1\text{MLCT}_1$ ,  ${}^1\text{MLCT}_2$  and  ${}^1\text{MLCT}_3$  as shown in Fig. 3. It can be noticed that these band maxima are separated by comparable energies (2300–2600  $\text{cm}^{-1}$ ), while the difference in energy between the band at 394 nm and  ${}^1\text{MLCT}_3$  is 3900  $\text{cm}^{-1}$ . This last band can be assigned to an MLCT transition involving a  $\pi_2^*$   $\text{H}_3\text{tcterpy}$  orbital in analogy with similar assignments done on  $C_2$  complexes of the type  $[\text{Os}(\text{bpy})_2(\text{X})_2]$  [16].

The three carboxylic functions on the terpyridine ligand can be deprotonated step by step by addition of TBAOH to give species with different absorption maxima. Fig. 4 shows the result of a spectrophotometric titration of a  $\text{CH}_3\text{OH}$  solution of  $[\text{Os}^{\text{II}}(\text{H}_3\text{tcterpy})(\text{CN})_3]^-$  with stoichiometric amounts of TBAOH. A progressive blue shift of all bands is observed upon going from the fully protonated form to the anionic species  $[\text{Os}^{\text{II}}(\text{tcterpy})(\text{CN})_3]^{4-}$ . These variations occurred with clear isosbestic points and can be interpreted in terms of delocalization of the carboxylate electronic charge on the terpyridine ring with the consequence of destabilizing the  $\pi^*$  orbitals thus giving a higher energy difference with the metal  $d\pi$  orbitals.

### 3.2. Electrochemistry

Oxidation potentials have been measured by means of cyclic voltammetry in  $\text{CH}_3\text{OH}$  solutions of the complexes using glassy carbon as working electrode and tetraethylammonium tetrafluoroborate 0.1 M as supporting electrolyte. The  $\text{Os}^{\text{II}} \rightarrow \text{Os}^{\text{III}}$  redox process was found to be reversible in all cases giving  $E_{1/2}$  values of 663, 605

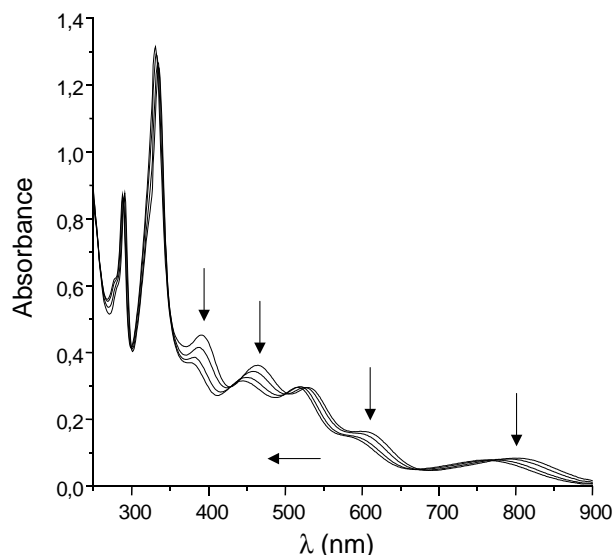


Fig. 4. Spectrophotometric titration of  $[\text{Os}^{\text{II}}(\text{H}_3\text{tcterpy})(\text{CN})_3](\text{TBA})$  with TBAOH in  $\text{CH}_3\text{OH}$ ; reported curves are related to the species  $[\text{Os}^{\text{II}}(\text{H}_3\text{tcterpy})(\text{CN})_3]^-$ ,  $[\text{Os}^{\text{II}}(\text{H}_2\text{tcterpy})(\text{CN})_3]^{2-}$ ,  $[\text{Os}^{\text{II}}(\text{Htcterpy})(\text{CN})_3]^{3-}$  and  $[\text{Os}^{\text{II}}(\text{tcterpy})(\text{CN})_3]^{4-}$  (arrows direction).

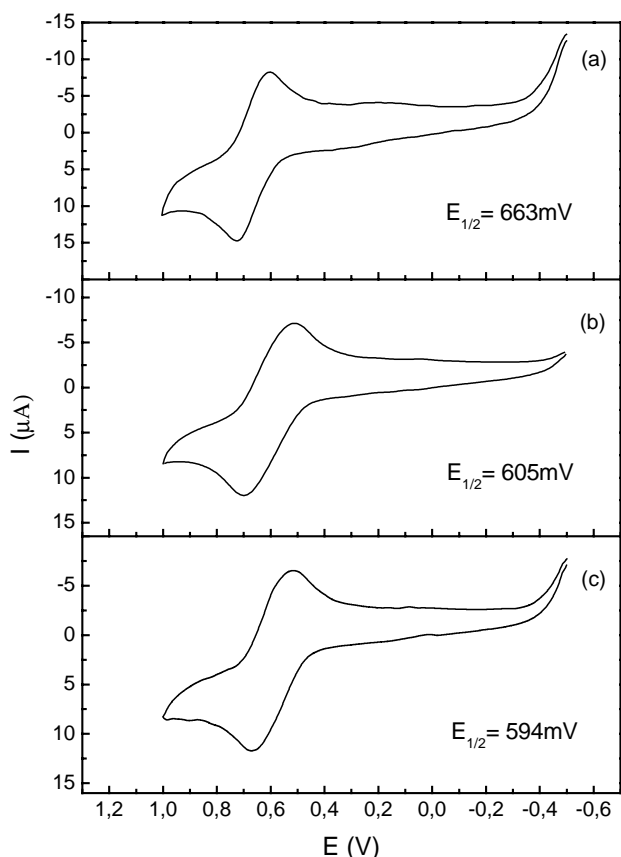


Fig. 5. Cyclic voltammograms of (a)  $[\text{Os}^{\text{II}}(\text{H}_3\text{tcterpy})(\text{CN})_2(\text{CNH})]$ , (b)  $[\text{Os}^{\text{II}}(\text{H}_2\text{tcterpy})(\text{CN})_3](\text{TBA})_2$  and (c)  $[\text{Os}^{\text{II}}(\text{Htcterpy})(\text{CN})_3](\text{TBA})_3$  in  $\text{CH}_3\text{OH}/\text{TEATFB}$  0.1 M using glassy carbon as working electrode.

and 594 mV for the species  $[\text{Os}^{\text{II}}(\text{H}_3\text{tcterpy})(\text{CN})_2(\text{CNH})]$ ,  $[\text{Os}^{\text{II}}(\text{H}_2\text{tcterpy})(\text{CN})_3](\text{TBA})_2$  and  $[\text{Os}^{\text{II}}(\text{Htcterpy})(\text{CN})_3](\text{TBA})_3$ , respectively (Fig. 5). The progressive shift at lower potential values upon deprotonation of the carboxylic

groups is in agreement with the destabilization effect of the negative carboxylate charge on terpy  $\pi^*$  orbitals which are therefore less effective to accept back-donation from the metal.

### 3.3. Photoelectrochemistry

The photoelectrochemical behavior of the osmium complex as a sensitizer in dye sensitized solar cells (DSSC) was tested both under monochromatic light and simulated solar radiation with respect to the known analogous ruthenium complex  $[\text{Ru}^{\text{II}}(\text{H}_3\text{tcterpy})(\text{NCS})_3]^-$  [19,20]. The photoaction spectrum obtained with DSSCs containing the species  $[\text{Os}^{\text{II}}(\text{H}_3\text{tcterpy})(\text{CN})_3]^-$  is reported in Fig. 6 and compared to that given by  $[\text{Ru}^{\text{II}}(\text{H}_3\text{tcterpy})(\text{NCS})_3]^-$ . The maximum monochromatic incident photon to current conversion efficiency (IPCE) attained with the Os sensitizer was around 50%, lower than that given by the triprotonated Ru complex. Nevertheless, the IPCE values above 900 nm were found to be slightly higher for the Os complex thanks to the contribution of the singlet–triplet band. Unlike the ruthenium complex, which shows a dependence of the sensitization performances on the degree of protonation [20], no significant differences in IPCE values were found in the case of the various protonated forms of the Os complex. Short-circuit photocurrent densities of  $11.1 \text{ mA cm}^{-2}$  were measured on devices with the Os sensitizer tested under AM1.5 simulated solar radiation. In the same experimental conditions a value of  $18.8 \text{ mA cm}^{-2}$  was found for the triprotonated Ru complex. Since photoanodes were of comparable absorbance ( $A > 1$ ) for all species, the LHE term cannot explain the difference in IPCE between the Os and the Ru sensitizers. The charge injection efficiency  $\phi$  and the collection efficiency  $\eta$  terms should therefore account for the observed data.

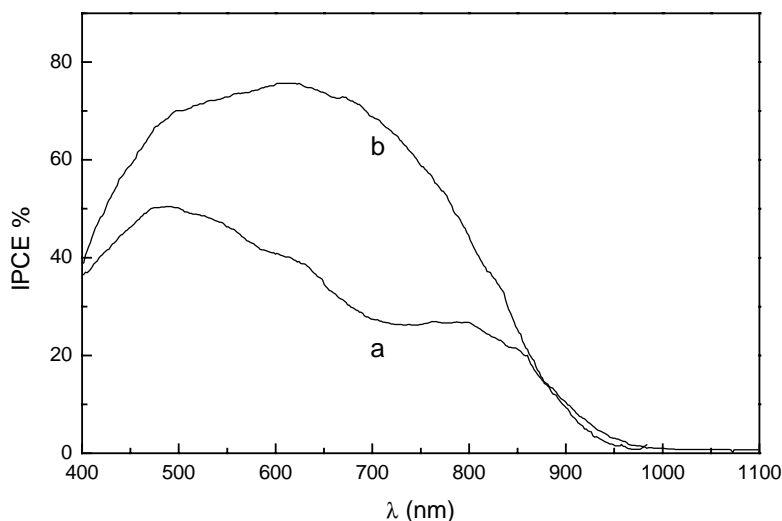


Fig. 6. Photoaction spectra of (a)  $[\text{Os}^{\text{II}}(\text{H}_3\text{tcterpy})(\text{CN})_3](\text{TBA})$  and (b)  $[\text{Ru}^{\text{II}}(\text{H}_3\text{tcterpy})(\text{NCS})_3](\text{TBA})$  on  $\text{TiO}_2$  electrodes with  $\text{LiI}$  2 M/ $\text{I}_2$  0.1 M in  $\gamma$ -butyrolactone as electrolyte.

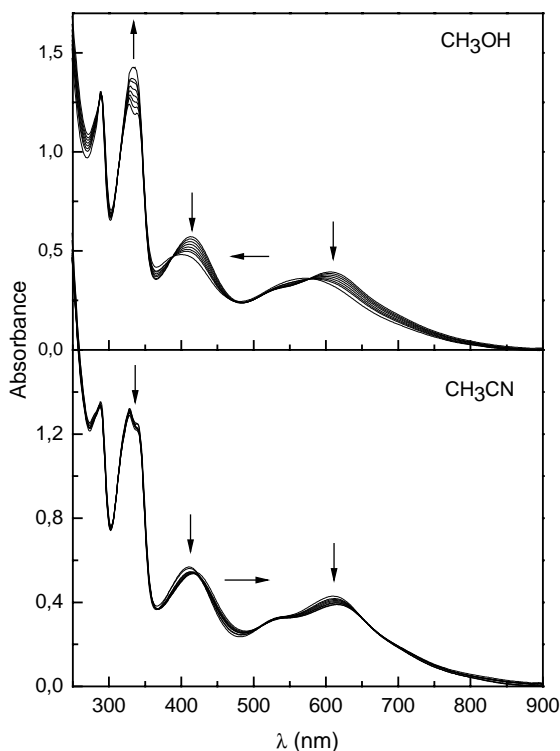


Fig. 7. Spectral variations of  $[\text{Ru}^{\text{II}}(\text{Htcterpy})(\text{NCS})_3](\text{TBA})_3$  irradiated at  $\lambda > 400$  nm in  $\text{CH}_3\text{OH}$  (upper curves) and  $\text{CH}_3\text{CN}$  (lower curves).

### 3.4. Photochemical stability

In order to investigate the suitability of the complex  $[\text{Os}^{\text{II}}(\text{Htcterpy})(\text{CN})_3]^{3-}$  as a sensitizer for long term application, the photochemical stability has been tested qualitatively both in  $\text{CH}_3\text{CN}$  and  $\text{CH}_3\text{OH}$  solutions irradiated with a Xe arc lamp at wavelengths  $>400$  nm. A comparison has been made, in the same experimental conditions, with the complex  $[\text{Ru}^{\text{II}}(\text{Htcterpy})(\text{NCS})_3]^{3-}$ . Samples of comparable absorbance were continuously irradiated for a period of up to 3 h in quartz spectrophotometric cuvettes with a path length of 1 cm, providing means for stirring and cooling. The Ru complex showed spectral changes with clear isosbestic points in both solvents resulting more unstable in  $\text{CH}_3\text{OH}$  where a blue shift of MLCT bands was observed (Fig. 7). The behavior in  $\text{CH}_3\text{CN}$  was the opposite with a red shift of MLCT bands during irradiation. The Os complex proved to be stable in both solvents in the time scale of these experiments. The higher stability of this Os complex is in line with the higher energy of the d–d states, with respect to the Ru case, known to be responsible of photochemical reactions in metal coordination compounds [16,17]. Although a detailed investigation, which is currently under way in our labs, is needed to clarify the photochemistry of the Ru complex, we can observe that the spectral variations are consistent with the formation of cyanide species, as it has been previously found in the case of the  $[\text{Ru}(\text{H}_2\text{dcb})_2(\text{NCS})_2]$  complex (dcb =

4,4'-dicarboxy-2,2''-bipyridine) [5]. Cyanide complexes are in fact strongly solvatochromic due to donor–acceptor interaction with the solvent [21], and in solvents with higher acceptor number [22] a decrease of the electronic density at the metal center is expected with a consequent blue shift of the MLCT bands.

## 4. Conclusion

A simple synthetic procedure has been devised for the preparation of the complex  $[\text{Os}^{\text{II}}(\text{H}_3\text{tcterpy})(\text{CN})_3]^-$  and more in general for complexes of formula:  $[\text{M}^{\text{II}}(\text{H}_3\text{tcterpy})(\text{X})_3]^-$  ( $\text{M}=\text{Ru}, \text{Os}$ ;  $\text{X}=\text{CN}^-, \text{NCS}^-, \text{Cl}^-$ , etc.). The Os complex shows an interesting structured UV-Vis spectrum, covering the whole visible region and part of near infrared, and a perfectly reversible electrochemistry. The presence of carboxylic functions on the chromophoric ligand  $\text{H}_3\text{tcterpy}$  allow for fine tuning of the electronic absorption and of the oxidation potential by simply changing the degree of protonation. The photoelectrochemical performances of the complex in DSSCs were tested and compared to those of the best known Ru sensitizer, yielding satisfactory IPCE values. The photochemical stability was checked in  $\text{CH}_3\text{OH}$  and  $\text{CH}_3\text{CN}$  and found to be superior to that of  $[\text{Ru}^{\text{II}}(\text{Htcterpy})(\text{NCS})_3]^{3-}$ . It can be concluded that the presented complex can be chosen as a model for the development of new osmium-based sensitizers, where spin-forbidden transitions could play a role in extending the spectral response in the NIR region for photoelectrochemical applications.

## Acknowledgements

This work was supported by IMRA Europe and by MIUR FIRB Project No. RBNE019H9K.

## References

- [1] (a) A. Hagfeldt, M. Graetzel, *Acc. Chem. Res.* 33 (2000) 269–277; (b) C.A. Bignozzi, M. Biancardo, P. Schwab, in: V. Ramamurthy, K.S. Schanze (Eds.), *Semiconductor Photochemistry and Photophysics*, Marcel Dekker, New York, 2003, pp. 1–49; (c) C.A. Bignozzi, J.R. Schoonover, F. Scandola, in: G.J. Meyer, K.D. Karlin (Eds.), *Molecular Level Artificial Photosynthetic Materials*, *Progress Inorganic Chemistry*, vol. 44, 1997, pp. 1–95.
- [2] F. Cecchet, A.M. Gioacchini, M. Marcaccio, F. Paolucci, S. Roffia, M. Alebbi, C.A. Bignozzi, *J. Phys. Chem.* 106 (2002) 3926–3932.
- [3] O. Kohle, M. Grätzel, A.F. Meyer, T.B. Meyer, *Adv. Mater.* 9 (1997) 904.
- [4] N.J. Cherepy, G.P. Smestad, M. Gratzel, J.Z. Zhang, *J. Phys. Chem. B* 101 (1997) 9342–9351.
- [5] (a) T. Hannappel, B. Burfeindt, W. Storck, F. Willig, *J. Phys. Chem. B* 101 (1997) 6799–6802; (b) J.E. Moser, D. Noukakis, U. Bach, Y. Tachibana, D.R. Klug, J.R. Durrant, R. Humphry-Baker, M. Gratzel, *J. Phys. Chem. B* 102 (1998) 3649–3650;

- (c) T. Hannappel, C. Zimmermann, B. Meissner, B. Burfeindt, W. Storck, F. Willig, *J. Phys. Chem. B* 102 (1998) 3651–3652.
- [6] G. Benko, P. Myllyperkio, J. Pan, A.P. Yartsev, V. Sundstrom, *J. Am. Chem. Soc.* 125 (2003) 1118–1119.
- [7] R. Argazzi, C.A. Bignozzi, G.H. Hasselmann, G.J. Meyer, *Inorg. Chem.* 37 (1998) 4533–4537.
- [8] H. Nusbaumer, J.E. Moser, S.M. Zakeeruddin, M.K. Nazeeruddin, M. Gratzel, *J. Phys. Chem. B* 105 (2001) 10461–10464.
- [9] S.A. Sapp, C.M. Elliott, C. Contado, S. Caramori, C.A. Bignozzi, *J. Am. Chem. Soc.* 124 (2002) 11215–11222.
- [10] B. O'Regan, D.T. Schwartz, S.M. Zakeeruddin, M. Gratzel, *Adv. Mater.* 12 (2000) 1263–1267.
- [11] Q.-B. Meng, K. Takahashi, X.-T. Zhang, I. Sutanto, T.N. Rao, O. Sato, A. Fujishima, H. Watanabe, T. Nakamori, M. Urugami, *Langmuir* 19 (2003) 3572–3574.
- [12] G. Sauvé, M.E. Cass, G. Coia, S.J. Doig, I. Lauermaun, K.E. Pomykal, N.S. Lewis, *J. Phys. Chem. B* 104 (2000) 6821–6836.
- [13] D. Kuciauskas, M.S. Friends, H.B. Gray, J.R. Winkler, N.S. Lewis, *J. Phys. Chem. B* 105 (2001) 392–403.
- [14] C.J. Barbe, F. Arendse, P. Comte, M. Jirousek, F. Lenzmann, V. Shklover, M. Gratzel, *J. Am. Ceram. Soc.* 80 (1997) 3157–3171.
- [15] C.A. Bignozzi, R. Argazzi, C. Chiorboli, F. Scandola, R.B. Dyer, J.R. Schoonover, T.J. Meyer, *Inorg. Chem.* 33 (1994) 1652–1659.
- [16] E.M. Kober, J.V. Caspar, R.S. Lumpkin, T.J. Meyer, *J. Phys. Chem.* 90 (1986) 3722–3734.
- [17] E.M. Kober, T.J. Meyer, *Inorg. Chem.* 21 (1982) 3967–3977.
- [18] K.D. Demadis, C.M. Hartshorn, T.J. Meyer, *Chem. Rev.* 101 (2001) 2655–2685.
- [19] Md.K. Nazeeruddin, P. Pechy, M. Graetzel, *Chem. Commun.* 18 (1997) 1705.
- [20] M.K. Nazeeruddin, P. Pechy, T.R. enouard, S.M. Zakeeruddin, R. Humphry-Baker, P. Comte, P. Liska, L. Cevey, E. Costa, V. Shklover, L. Spiccia, G.B. Deacon, C.A. Bignozzi, M. Graetzel, *J. Am. Chem. Soc.* 123 (2001) 1613–1624.
- [21] C.J. Timpson, C.A. Bignozzi, B.P. Sullivan, E.M. Kober, T.J. Meyer, *J. Phys. Chem.* 100 (1996) 2915–2925.
- [22] V. Gutmann, *The Donor–Acceptor Approach to Molecular Interactions*, Plenum Press, New York, 1980.